Enviado para publicar por Elsevier: Chemical Engineering Science 57 (2002) 2381 – 2393

Calcination of calcium –based sorbents at pressure in a broad range of CO_2 concentrations

F. García-Labiano, A. Abad, L .F. de Diego, P. Gayán, J. Adánez[*]

Instituto de Carboquímica (C.S.I.C), Department of Energy and Environment

Miguel Luesma Castán 4, 50015. Zaragoza, Spain

Abstract

The calcination reaction of two limestones and a dolomite with different porous structures was studied by thermogravimetric analysis. The effects of calcination temperature (1048-1173 K), particle size (0.4-2.0 mm), CO_2 concentration (0-80 %) and total pressure (0.1-1.5 MPa) were investigated. SEM analysis indicated the existence of two different particle calcination models depending on the sorbent type: a shrinking core model with a sharp limit between the uncalcined and calcined parts of the particle and a grain model with changing calcination conversion at the particle radial position. The appropriate reaction model was used to determine the calcination kinetic parameters of each sorbent. Chemical reaction and mass transport in the particle porous system were the main limiting factors of the calcination reaction at the experimental conditions. A Langmuir-Hinshelwood type kinetic model using the Freundlich isotherm was proposed to account the effect of the CO_2 during sorbent calcination. This allowed us to predict the calcination conversion of very different sorbents in a broad range of CO_2 partial pressures. Total pressure also inhibited the sorbent calcination. This fact was accounted by an additional decrease in the molecular diffusion coefficient with increasing total pressure with respect to the indicated by the Fuller's equation.

Keywords: Calcination; Pressure; Environment; Kinetics; Modelling; Reaction engineering

[*] Corresponding author: Tel: (34) 976733977; fax: (34) 976733318. *E-mail address*: jadanez@carbon.icb.csic.es (J. Adánez)

1. Introduction

The understanding of thermal calcium carbonate decomposition kinetic and reaction mechanism has been the object of many studies over the years because of his multiple practical and industrial applications. The operating conditions are largely influenced by the lime use. Quicklime necessary for metal refining, cement, calcium carbide synthesis and soil stabilisation is produced in lime kilns. These kilns are operated at high temperatures (1473-1673 K) and the fed particles are in a wide size range from 2 mm to 15 mm. Other important use of lime is related with environmental applications necessary in many coal-based power plants, especially to retain sulphur-derived pollutants. In this case, the decomposition reaction of the limestone is influenced by the presence of SO_2 or H_2S because calcination and desulfurization take place simultaneously. The operating conditions depend on the system used for coal processing. Temperatures from 873 to 1673 K and particle sizes in the 5-90 μm interval are normal in furnace sorbent injection processes during pulverised coal combustion. Lower temperatures, about 1123 K, and higher particle sizes, up to 4 mm, are used in fluidised bed combustors. The CO_2 content in exhaust combustion gases varies from 10 to 15%. The calcium-based sorbent can decompose also at higher CO_2 partial pressures in those processes working at high pressure, as in the integrated gasification combined cycle (IGCC) process. In all the above systems, the calcination conditions have an important effect, either because of differences in lime particle properties or because of reaction rate limitations.

However, there are many aspects not well understood about the calcination reaction, and therefore there is no consensus about several fundamental aspects of the process as particle reaction model, rate-limiting processes, and influence of the CO_2 partial pressure, and total pressure on the reaction rate.

Several investigations (Ingraham & Marier, 1963; Fuertes, Marbán & Rubiera, 1993a) have shown that the decomposition of the calcium carbonate occurs at a definite boundary between the CaO and $CaCO_3$ phases, which moves at a constant rate towards the centre of the particle. Dennis & Hayhurst (1987) and Silcox, Kramlich & Pershing (1989) used this particle reaction model, the shrinking core model, to predict their experimental results. On the other hand, Borgwardt (1985) assumed a homogeneous

reaction throughout the sorbent with particle sizes under 90 μm. Khinast, Krammer, Brunner & Staudinger (1996) concluded that simple particle models such as the Shrinking Core Model (SCM) and the Uniform Conversion Model (UCM) could only be correctly applied to extreme cases. Rao, Gunn & Bowen (1989) assumed a gradual conversion in the pellets of about 6.5 mm size with the mass transfer in the porous system controlling the reaction. Later, Hu & Scaroni (1996) observed by SEM analysis different conversion levels inside the particle in partially calcined limestone of 63 μm size.

Three possible rate limiting processes involved in the decomposition of calcium-based sorbents can be distinguished inside the particle: (1) heat transfer through the particle to the reaction interface, (2) mass transfer of the CO_2 released from the reaction surface through the porous system, and (3) chemical reaction. External mass transfer could be also a rate-limiting process in some cases. The relative importance of the different limiting steps on the overall reaction may be largely due to experimental conditions, experimental set-up, and sample size.

Since the calcination is an endothermic reaction, temperature in the calcination zone of the particle decreases and a heat transfer process occurs from the particle surroundings to that zone. The relative importance of the heat transfer process is greatly influenced by particle size (Khinast et al., 1996; Hu & Scaroni, 1996; Fuertes, Alvarez, Rubiera, Pis & Marban, 1993b). However, mass transfer and chemical reaction have been considered as the rate limiting processes by the majority of the authors.

There are also different opinions about the effect of CO_2 on the calcination rate. Ingraham & Marier (1963) found that the reaction rate depended linearly on the difference between the CO_2 pressure at the reaction surface and the equilibrium pressure. Several authors (Silcox et al., 1989; Khraisa & Dugwell, 1989; Fuertes et al. 1993a) have later used this relation to fit their results. Ohme, Schrader & Müller (1975) mentioned that the reaction rate coefficient was inversely proportional to the CO_2 partial pressure. Following the same idea, Khinast et al. (1996) found an exponential decay in reaction rate constant with the CO_2 pressure. Hashimoto (1962) reported that the rate dependency on CO_2 partial pressure was linear at lower temperatures and non-linear at higher temperatures. Rao et al. (1989) also found a non-linear dependency at 953-1148

K with the degree of non-linearity dependent on temperature. Darroudi & Searcy (1981) found that at low CO_2 partial pressures the rate was essentially independent of the partial pressure, whereas at higher values there was a parabolic dependency, which changed to linear for values near to the thermodynamic equilibrium. It is clear that the reaction at the interface $CaCO_3$-CaO is complex and not fully understood. Several workers have suggested that the non-linear dependence found for the effect of CO_2 on the calcination rate could be due to the existence of a sorption process at the calcination surface (Hyatt, Cutler & Wadsworth, 1958; Wang & Thomson, 1995; Khinast et al., 1996).

Few previous works have considered the effect of total pressure on the calcination rate of sorbents. Dennis & Hayhurst (1987) found that the rate of calcination was slower at higher pressures, even when there was not present CO_2 in the bulk gases. This effect was considered by assuming that exists a spurious partial pressure of CO_2 at equilibrium lower than the obtained from thermodynamic data and which depends on temperature and total pressure. They recognised that it was difficult to justify the use of a spurious pressure, but it did account satisfactorily for their results. Other works have also found non-usual effects of total pressure on the rate of different reactions, as for example, sulfidation of calcium-based sorbents (Matsukata, Ando & Ueyama, 1999) and stabilisation of sulphided sorbents (Yrjas, Hupa & Iisa, 1996). They related this effect with a possible inhibition of intraparticle diffusion of gases at high total pressures. However, the reason for the influence of total pressure on a gas-solid reaction rate is still not clear.

Although several attempts have been made to produce a mathematical model to account for the observed effects in calcium sorbent calcination, none has been demonstrated to be valid over a wide range of CO_2 concentrations and total pressures. The objective of this work is to develop a particle model able to adequately predict the calcination rate of the most usual calcium-based sorbents in a wide range of operation conditions as temperature, CO_2 partial pressure and total pressure. For this purpose, two limestones with different physical and chemical properties, and a dolomite have been used. Scanning Electron Microscopy (SEM) analysis of the samples has been used to elucidate the particle reaction model followed by the different sorbents.

2. Experimental

2.1. Apparatus

Two different thermobalance have been used to work either at atmospheric or pressure conditions. For the experiments carried out at atmospheric pressure, a Thermo-Gravimetric Analyser (TGA) Setaram TGC-85 type was used. The desired reactant gas mixture, prepared by blending CO_2 and N_2 streams, was introduced at the bottom of the reaction quartz tube (15 mm I.D.).

A Cahn TG-2151 thermobalance was used for the pressurized experiments. The thermobalance can be used up to 10 MPa and 1373 K. A quartz tube (31 mm I.D.) located at the inner of the pressure furnace was used as a reactor. The latter was vertically moved by means of an elevator and joined to the TG-head by means of a clamp. Nitrogen flowed through the TG-head and between the pressure furnace vessel and the quartz tube to prevent corrosion. A thermocouple was located just a few millimetres below the sample-holder, inside the reactor.

The sample-holder was a wire mesh platinum basket (11 mm diameter, 4 mm height, and 0.25 mm of wire mesh size) to avoid corrosion and reduce mass transfer resistance around the sorbent sample. Temperature and sample weight were continuously collected and recorded in a computer. The reacting gas mixture (83 cm^3/s s.t.p.), containing N_2 and CO_2 in the desired ratio, was measured and controlled by electronic mass flow controllers and was introduced at the bottom of the reaction tube.

2.2. Materials

Two limestones, Blanca and Mequinenza, and a dolomite, Sierra de Arcos, were used in four narrow particle size intervals between 0.4 and 2 mm. The chemical analyses and physical characteristics of these sorbents are shown in Table 1. The limestones were selected due to their very different initial porosity, which could affect their calcination reactivity. The porosity and specific surface area of CaO corresponds to samples calcined in nitrogen at 900 ºC and cooled just after finish the process.

2.3. Procedure

(a) Atmospheric experiments. Calcination of sorbents was carried out at temperatures from 1048 K to 1173 K. Several CO_2 concentrations (between 0 and 80%) in the reactant gas, and different sorbent particle sizes (+0.4-0.63 mm, +0.8-1.0 mm, +1.25-1.6 mm, and +1.6-2 mm) were used. For each run, about 10 mg of sample was put into the basket and rapidly introduced into the furnace at the desired calcination temperature in pure CO_2 atmosphere to prevent calcination before heating sample. The decomposition is initiated by a change of the gas composition to the desired CO_2/N_2 ratio. No appreciable effect of the change of gases was observed in calcination behaviour. The calculus of the axial dispersion coefficient gave values of D/uL lower than 0.01, which confirmed the existence of gas plug flow in the reactor. The total gas feed rate in the reaction zone was 3.9 cm^3/s (s.t.p.). This value corresponds to a gas velocity of 0.09 m/s at 1123 K. For the dolomite, the reactant gas was introduced just after finishing the calcination of the $MgCO_3$, which took place even in pure CO_2 atmosphere.

(b) Pressurised experiments. To analyse the effect of total pressure on the sorbent calcination rates the following basic conditions were chosen: 1 MPa of total pressure, 1123 K, and 0% of CO_2. Later, the effect of the different operating conditions was studied. For each run, about 10 mg of sample was placed into the basket at room temperature. The thermobalance was first pressurized to the desired pressure and then heated up to the desired temperature at 20 K/min in a CO_2 atmosphere to prevent sorbent from decomposition. The reactant gas was then switched to obtain the desired CO_2/N_2 ratio and the weight change measurement was recorded in the computer. The total gas feed rate in the reaction zone was 83 cm^3/s (s.t.p.). This value corresponds to a superficial velocity of 0.45 m/s at 1123 K and atmospheric pressure. Calcination of the $MgCO_3$ contained in the dolomite started during sample heating in CO_2 and had finished before switch the gas to the desired CO_2/N_2 ratio. When dolomite is immediately exposed to a high temperature a two steps process can be also considered taken into account that $MgCO_3$ decomposes quicker than the $CaCO_3$ (Dennis and Hayhurst, 1987). Therefore, the decomposition of the $MgCO_3$ only produces a small delay in the beginning of the $CaCO_3$ decomposition under usual operating conditions.

Experiments with different sample weights and gas flowrates were carried out to detect the importance of the external mass transfer and the interparticle diffusion in the

experimental system. The linear velocity into the reactor and operating conditions used in the atmospheric pressure TG experiments were enough to avoid the influence of these resistances. On the other hand, Figure 1 shows the results obtained with different sample weights and gasflowrates with Blanca limestone particles working at pressure. It can be observed that the intraparticle mass resistance was avoided with sample weights under 25 mg. However, the great decrease produced in the gas velocity at increasing pressure made very difficult to avoid the external mass transfer even when working at the highest gas flowrate admissible by the system. It must be taken into account that higher flowrates produced too much noise in the weight electronic signal to be acceptable. Therefore, a sample weight of 10 mg and the highest gas flowrate possible, 83 cm^3/s (s.t.p) were used in the pressurised thermobalance. In this case, the external mass transfer must be considered in the analysis of the experimental results.

2.4. SEM analysis

To elucidate the behaviour of the calcination reaction in the sorbent particles, several samples of the two limestones and the dolomite partially calcined at roughly 50% were analysed by SEM. The sample preparation was carried out in a inert atmosphere chamber to avoid the hydration of the CaO. The samples were put on top of a resin sample holder, embedded in a drop of epoxy-resin, left overnight, introduced in liquid nitrogen and then fractured to obtain a fresh surface in which well-preserved particle cross-sections could be observed. The samples were cleaned with air to avoid the possible water condensation at the surface and then introduced into a dessicator. A cut previously made to the sample holder in a direction crossing the hardened resin drop (but not reaching it) ensured that the fracture affected the region containing the sample. The backscattered electron signal provided sufficient phase contrast between sample and resin for the recognition and image processing of particle cross-sections.

3. Calcination particle model

To elucidate the particle reaction model of our sorbents, some samples were partially calcined at 1123 K in nitrogen atmosphere and analysed by SEM. Figure 2 shows different micrographs of the limestones and dolomite used in the work. Figures

2a and 2b show the results obtained with the Blanca limestone. The limit between the uncalcined and calcined parts of the particle can be clearly distinguished. The $CaCO_3$ phase is characterised by large and regular crystals, whereas the CaO phase is more disperse. Figures 2c and 2d show the external and internal micrographs of the partially calcined Mequinenza limestone, respectively. Figure 2c shows a well developed and sintered CaO grains. In Figure 2d it can be observed grains of CaO in the surrounding of a large $CaCO_3$ grain, indicating that calcination also exists in the centre of the particle. Figures 2e and 2f show a general picture and a more detailed view of a partially calcined particle of dolomite. Although two different zones seems to be identified in Figure 2e, the external zone corresponds to resin introduced during sample preparation. A detailed analysis of the particle revealed the existence of a homogeneous granular texture throughout the particle and the existence of some calcination in several locations inside the particle. Since no differences in structure were found in different zones it can be assumed that calcination took place over the whole particle.

The results obtained by the SEM micrographs confirmed the existence of two different particle reaction models. Blanca limestone followed a shrinking core model. In contrast, a reaction model with different calcination conversion at different particle positions should be used for Mequinenza limestone and the Sierra de Arcos dolomite. Due to the granular structure of the solid matrix observed in these samples, a grain model with internal diffusion resistance was developed and used for these sorbents. The different calcination behaviour observed could be due to differences in sorbent porosity. As can be seen in Table 1, half-calcined dolomite ($CaCO_3 \cdot MgO$) and Mequinenza limestone exhibited high porosity, whereas Blanca limestone had a very low porosity.

To determine the kinetic parameters of the calcination reaction a changing grain size model was used for Mequinenza limestone and Sierra de Arcos dolomite, whereas a shrinking core model was used for Blanca limestone. Moreover, previous calculations revealed that heat transfer was not a rate-limiting factor to the sorbent calcination within the operating conditions used in this work. The relative influence of the other possible rate-limiting factors, pore diffusion inside the particle and chemical reaction, will depend on the temperature, CO_2 concentration, total pressure, and particle size. Although the operating conditions selected for the atmospheric pressure experiments

avoided the external mass transfer resistance, this process can have a relative importance during high pressure runs and therefore will be considered in the models.

3.1. Changing grain size model (CGSM)

Grain models assume that the solid structure consists of a matrix of very small grains, usually spherical in shape. In this section, the changing grain size model proposed by Georgakis, Chang & Szekely (1979) has been adapted to the specific case of the calcination reaction. This model assumes that the particle consists of a number of non-porous spherical grains of uniform initial radius, r_0. SEM micrographs of Mequinenza limestone and Sierra de Arcos dolomite revealed that the product CaO formed small grains around the unreacted core grain $CaCO_3$ (see Figure 2d). Therefore, the unreacted core radius of $CaCO_3$, r_2, that at t=0 is r_0, shrinks as the reaction proceeds while the CaO product generates a porous structure as consequence of its lower molar volume with respect to the original $CaCO_3$.

The calculation of the overall reaction rate in terms of the solid conversion as a function of time requires the solution of the following equations with appropriate boundary conditions: (1) a differential mass balance equation for the gas diffusion and reaction within the particle, which yields the gas concentration profile through the particle; and (2) an equation for the movement of reaction interface inside the grains, which is determined from the chemical reaction rate taking place at the reaction interface.

For the resolution of the model, the pseudo-steady state hypothesis for the gas concentration profile in the particle and some assumptions have been used. The solid reactant is considered as an isothermal spherical particle. Although the shrinkage in volume of calcined samples ranges from 9 to 14 % (Fuertes, Alvarez, Rubiera, Pis & Marban, 1991) this represents only a shrinkage in diameter from 3 to 5%, and no change in size has been considered. Moreover, the effect of sintering has not taken into account. Sintering is a process that produces a reduction in the specific surface area of CaO, specially in the first moments of the reaction, although maintains constant the porosity (Fuertes et al., 1991). The specific surface area of the CaO changes from the nascent value 104 m^2/g, (Borgwardt,1985), to about 15-30 m^2/g in the first moments of the decomposition and then decreased to an asymptotic value at infinite time. This

phenomena is very important in those processes where the time scales of sorbent decomposition and reaction are similar as for example, the calcination-sulphation in furnace sorbent injection processes. However, the surface of the CaO generated during calcination slightly affects to the calcination reaction by the change in the effective diffusivity of gas inside the sorbent. In this work, a value of specific surface area of CaO corresponding to particles just after calcination has been used.

The mass balance for diffusion and reaction of the gas over a differential volume element in a spherical particle, assuming the pseudo steady-state, is given by the following differential equation:

$$\frac{1}{R^2}\frac{\partial}{\partial R}\left(D_e R^2 \frac{\partial P_{CO_2}}{\partial R}\right) - (r)_c' = \frac{\partial P_{CO_2}}{\partial t} = 0 \qquad (1)$$

The boundary conditions required for the solution of this equation, when external mass transfer is affecting the overall reaction rate, are the following:

$$-D_e \frac{\partial P_{CO_2}}{\partial R} = k_g\left(P_{CO_2} - P_{bulk}\right) \qquad \text{at} \quad R = R_0 \qquad \text{and} \geq t \quad 0 \qquad (2)$$

$$\frac{\partial P_{CO_2}}{\partial R} = 0 \qquad \text{at} \quad R = 0 \qquad \text{and} \geq t \quad 0 \qquad (3)$$

Although the way to calculate the external mass transfer coefficient is not clearly defined for TG experiments, k_g was calculated by means of the Sherwood number (Schlichting, 1979) as

$$Sh = \frac{k_g d_p}{D_{CO_2}} = 2 + 0.6 \cdot Re_p^{1/2} \cdot Sc^{1/3} \qquad (4)$$

The reaction rate per unit of particle volume is proportional to the chemical reaction rate constant, k_c, the reaction surface, S_e, and a function of the CO_2 partial pressure. The form of the CO_2 partial pressure function is discussed below.

$$(r)_c = k_c \cdot S_e \,.f(P_{CO_2}) = k_c \cdot S_0 (r_2/r_0)^2 \,.f(P_{CO_2}) \qquad (5)$$

The initial condition for this equation is $r_2 = r_0$ and $S_e=S_0$ at t = 0. The initial radius of the grains, r_0, within a certain particle can be derived from the relationship:

$$r_0= 3\,(1-\varepsilon_0)/S_0 \tag{6}$$

The radius of the unreacted grain core, r_2, at each time and position inside the particle is calculated with the equation:

$$\frac{dr_2}{dt} = k_c \cdot V_{M,CaCO_3} \cdot f(P_{CO_2}) \tag{7}$$

The effective diffusivity is calculated as a function of the particle porosity by:

$$D_e = D_g \varepsilon^2 \tag{8}$$

The porosity changes inside the particle with calcination conversion were calculated as a function of the initial porosity, ε_0, and the stoichiometric volume ratio of solid product to solid reactant, Z:

$$\varepsilon(R,t) = \varepsilon_0 - (Z-1)(1-\varepsilon_0)X(R,t) \tag{9}$$

where Z is defined as:

$$Z = 1 + \frac{\rho_{r,CaCO_3}\left(V_{M,CaO} - V_{M,CaCO_3}\right)}{M_{CaCO_3}} \tag{10}$$

The gas diffusivity depends on the type of gas diffusion in the pores. Due to the variation in the size of the pores during the calcination reaction, the gas diffusivity was calculated as a combination of the molecular and Knudsen diffusions:

$$D_g = \left[D_{CO_2}^{-1} + D_K^{-1}\right]^{-1} \tag{11}$$

Knudsen diffusivity was calculated using the following equation:

$$D_K = 97\, r_p \sqrt{\frac{T}{M_{CO_2}}} \tag{12}$$

being

$$r_p = 2\frac{\varepsilon}{S_e} \tag{13}$$

The specific surface area of the sorbent, S_e, was function of the particle conversion level,

$$S_e = \left[S_{g,CaO}X + S_{g,CaCO_3}(1-X)\right]\left[\frac{X}{\rho_{r,CaO}} + \frac{1-X}{\rho_{r,CaCO_3}}\right]^{-1}(1-\varepsilon) \tag{14}$$

The molecular diffusivity of CO_2 in N_2 is calculated using the equation proposed by Fuller, Schettler & Giddings (1966):

$$D_{CO_2} = \frac{10^{-7}\, T^{1.75}\,(M_{CO_2}^{-1} + M_{N_2}^{-1})^{0.5}}{P\left[(\Sigma v)_{CO_2}^{1/3} + (\Sigma v)_{N_2}^{1/3}\right]^2} \tag{15}$$

The local conversion at each time and position inside the particle was calculated with the equation:

$$X(R,t) = 1 - \left[\frac{r_2(R,t)}{r_0}\right]^3 \tag{16}$$

The mean conversion at each time in the whole particle was calculated by integration of local conversions,

$$X(t) = \frac{\int_0^{R_0} 4\pi R^2 X(R,t)\,dR}{\frac{4}{3}\pi R_0^3} \tag{17}$$

3.2. Shrinking core model (SCM)

The shrinking core model considers the decomposition of the $CaCO_3$ at a well-defined CaO-$CaCO_3$ interface around the particle and the diffusion of the CO_2 released through the porous CaO to the particle surface. The sorbent particle has been assumed to be spherical and isothermal.

The equation governing the movement of the calcination was:

$$\frac{dR_c}{dt} = -k_c V_{M_{CaO}} f(P_{CO_2}) \qquad (18)$$

with $R_c = R_0$ at $t = 0$. The differential equation governing the diffusion of CO_2 through the porous lime was:

$$\frac{\partial^2 P_{CO_2}}{\partial R^2} + \left(\frac{2}{R} + \frac{1}{D_e} \frac{\partial D_e}{\partial R} \right) \frac{\partial P_{CO_2}}{\partial R} = \frac{1}{D_e} \frac{\partial P_{CO_2}}{\partial t} \qquad (19)$$

with two boundary conditions:

$$-D_e \frac{\partial P_{CO_2}}{\partial R} = k_g \left(P_{CO_2} - P_{bulk} \right) \qquad \text{at} \qquad R = R_0 \qquad (20)$$

$$-\frac{D_e}{R_g T} \frac{\partial P_{CO_2}}{\partial R} = k_c \, f\left(P_{CO_2} \right) \qquad \text{at} \qquad R = R_c \qquad (21)$$

Applying the pseudo-steady-state approximation for gas-solid reactions, and considering D_e as constant with time, equation (19) can be simplified to:

$$\frac{\partial^2 P_{CO_2}}{\partial R^2} + \frac{2}{R} \frac{\partial P_{CO_2}}{\partial R} = 0 \qquad (22)$$

The movement of the calcination front and the radial profiles of CO_2 were calculated using the numerical solution procedure proposed by Silcox et al. (1989).

4. Results and discussion

To calculate the kinetic parameters of the calcination reaction for the different sorbents, several experiments were first carried out at atmospheric pressure. Later, the effect of total pressure on the calcination rate was considered.

4.1. Effect of temperature

Calcination experiments of the three sorbents with particle sizes of 0.8-1 mm were carried out at atmospheric pressure and temperatures from 1048 to 1173 K in nitrogen atmosphere. As expected, the calcination rate increased with temperature in all

of the range tested and for all sorbents. The calcination rate of Mequinenza limestone and Sierra de Arcos dolomite were high and very similar. However, the calcination rate of Blanca limestone was slower due to their lower porosity and high crystalline structure.

4.2. Effect of CO_2 partial pressure

Atmospheric experiments were also carried out to determine the effect of the CO_2 partial pressure on the calcination rate of the sorbents. Several CO_2 partial pressures between 0 and 80 % were used at different temperatures from 1073 to 1173 K. Figure 3 shows some examples of the conversion versus time curves for the two limestones and the dolomite at different CO_2 partial pressures and temperatures. An increase in the CO_2 partial pressure produced always a clear decrease in the calcination rate. This decrease was especially high for the highest CO_2 partial pressures, corresponding to about the 80 % of the maximum allowed by the thermodynamic equilibrium.

To find the relation between the calcination rate and the CO_2 partial pressure, two different expressions were tested:

$$f\left(P_{CO_2}\right) = \exp\left(-a\frac{P_{CO_2}}{P_{eq}}\right) \tag{23}$$

$$f\left(P_{CO_2}\right) = \left(1-\frac{P_{CO_2}}{P_{eq}}\right)^{b} \tag{24}$$

Equation (23) was proposed by Khinast et al. (1996), and equation (24), with the exponent “b” ranging from 1 to 2, has been used by several authors (Rao et al., 1989; Silcox et al., 1989; Fuertes et al., 1993a; Hu & Scaroni, 1996) to adequately describe the calcination rate of their sorbents. All of them worked in a narrow range of CO_2 concentrations. These equations were used together with the corresponding particle model, SCM or CGSM, to fit the experimental conversion versus time curves obtained with the three sorbents. In this way, it was possible to obtain the kinetic parameters of the calcination reaction. The Nelder & Mead (1964) method was used to obtain the best values of the kinetic parameters and the constants “a” and “b” of equations (23) and

(24). As an example, Figure 4 shows a comparison between the experimental data with Blanca limestone and model predictions. Both equations were valid to predict the calcination conversions in a limited range of CO_2 concentrations although clearly overpredicted the experimental data at the highest CO_2 concentrations.

Khinast et al. (1996) indicated that there was no proper explanation for the exponential decay of calcination rate with CO_2 partial pressure. They suggested possible sorption effects at the $CaCO_3$ surface as a possible cause for this exponential dependence. Other workers have also indicated the possible existence of a sorption process in the calcination reaction. Hyatt et al. (1958) presented a model based on chemical reaction limitations where an intermediate product was formed on the reaction surface. Dennis & Hayhurst (1987) concluded that very complex processes must occur at the reaction interface, which include the breakdown of the rhombohedral $CaCO_3$ lattice, followed by the desorption of CO_2, and the nucleation and growth of cubic CaO. Wang & Thomson (1995) also explained with a sorption mechanism the effect of H_2O on the calcination rate of a sorbent.

Following this idea, a Langmuir-Hinshelwood mechanistic model was used to describe the chemical reaction accounting for the sorption of CO_2 on the $CaCO_3$ surface.

1. Chemical decomposition of $CaCO_3$ to give CaO and adsorbed CO_2.

$$CaCO_3 + n\,L \underset{k_2}{\overset{k_1}{\rightleftharpoons}} CaO + n\,L(CO_2) \qquad K_1=k_1/k_2 \qquad (25)$$

where $n\,L(CO_2)$ accounts for one CO_2 molecule chemisorbed on “n” active sites “L”. In adsorption processes, “n” usually varies between 0 and 2.

2. Desorption of adsorbed CO_2.

$$n\,L(CO_2) \underset{k_A}{\overset{k_D}{\rightleftharpoons}} n\,L + CO_2 \qquad K_A=k_A/k_D \qquad (26)$$

Obviously, the overall calcination reaction is:

$$CaCO_3 \rightleftharpoons CaO + CO_2 \qquad (27)$$

The equilibrium constant of reaction (27) was obtained from thermochemical data (Barin, 1989):

$$K_{eq} = P_{eq} = 4.137 \cdot 10^{12} \exp\left(-\frac{20474}{T} \right) \quad (28)$$

When the reaction is controlled by chemical decomposition, reaction (25), the reaction rate per unit of particle volume is given by:

$$(r)_c = k_c \cdot S_e \cdot (1-\theta) \cdot \left(1 - \frac{P_{CO_2}}{P_{eq}} \right) \quad (29)$$

where θ is the fraction of active sites occupied by CO_2. In these conditions, θ is given by the appropriate adsorption isotherm. Two adsorption isotherms have been tested in this work.

$$\theta = \frac{\left(K_A P_{CO_2} \right)^{1/n}}{1 + \left(K_A P_{CO_2} \right)^{1/n}} \quad (30)$$

$$\theta = c \cdot P_{CO_2}^{1/n} \quad (31)$$

$$c = c_0 \, e^{(-E/RT)} \quad (32)$$

Equation (30) is a modified Langmuir isotherm to account for the active sites occupied by one molecule of CO_2. When n=1, this equation corresponds to the Langmuir isotherm, the most commonly used in the literature. Equation (31) is the Freundlich isotherm. Although power law models do not always lack mechanistic realism, this type of isotherms can certainly be accepted wherever they are found to fit the data (Doraiswamy & Sharma, 1984). K_A and c are adsorption constants, which are dependent on temperature.

The modified Langmuir isotherm has been used with the particle models above described with different values of the exponent “n” ranging between 0.5 and 2. The equation was valid for low CO_2 concentrations although the theoretical calcination rate overpredicted the experimental results at the highest CO_2 partial pressures, similarly to the behaviour obtained with equations (23) and (24).

Freundlich isotherm was also used to fit experimental conversion vs. time curves at different CO_2 partial pressures. The best fit was found for "n" equal to 2. The theoretical conversion versus time curves obtained with the Freundlich isotherm combined with the particle reaction models are plotted as continuous lines in Figure 3 for different sorbents, temperatures and CO_2 partial pressures. A good agreement between measured and predicted data can be observed in all range of CO_2 partial pressures working at atmospheric pressure. This indicates that the mechanistic adsorption model suggested in reactions (25) and (26) using the Freundlich isotherm is valid to describe the calcination reaction in a broad range of CO_2 partial pressures.

This adsorption mechanism, together with the corresponding particle model (SCM or CGSM), was used to determine the values of the chemical reaction rate constant, k_c, and the adsorption constant, c, for each sorbent and temperature. An Arrhenius type dependence with temperature was assumed for both parameters. Figures 5 and 6 show the Arrhenius plots for the two limestones and the dolomite, and Table 2 shows the values of the preexponential factors and activation energies obtained in each case.

The very similar values of the adsorption constant, c, obtained for the two limestones and the dolomite, could indicate a similar surface chemisorption process for the three solids tested. On the other hand, the E_c values were in the range obtained by other authors in similar experimental conditions. The activation energies obtained for limestone calcination in a thermogravimetric analyser or in a differential reactor with big particle sizes and temperatures under 1173 K varied between 110 and 204 kJ mol^{-1} (Borgwardt, 1985; Rao et al., 1989; García-Calvo, Arranz & Letón, 1990).

For comparison purposes, the results obtained by other authors were also plotted in Figure 5. Borgwardt (1985) used the uniform conversion model (UCM) to obtain calcination kinetic data by using small particles, 1-90 μm. These data have been widely adopted later by other authors. We can see in the figure that the kinetic constants of Blanca limestone are higher and the data of Mequinenza limestone and the dolomite are smaller than the obtained by Borgwardt (1985). Assuming the calcination parameters obtained by Borgwardt (1985) are intrinsic kinetic data, the calcination differences between several calcium sorbents must be due to the reaction surface. This would indicate that not all the surface area given by the CGSM is active for reaction in the

Mequinenza limestone and the dolomite. In contrast, for Blanca limestone, the surface of the reaction interface $CaCO_3$-CaO should be higher than the defined by the surface of a sphere in the SCM, as proposed by Fuertes et al. (1993a).

As the CGSM takes into account all the surface area available for reaction, this model was used to predict the data obtained by Fuertes et al. (1993a). The conversion versus time curves predicted by the CGSM were nearly identical to the SCM predictions and the kinetic parameters obtained in this case were similar to the given by Borgwardt (1985), as can be observed in the figure. Obviously, very sharp profiles were predicted inside the sorbent, close to the showed by a SCM. Similarly, the Blanca limestone data were fitted by using the CGSM and the kinetic results obtained were close to the obtained by Borgwardt (1985), although the quality of the fit in the conversion versus time curves made worse.

The CGSM was also valid to predict the conversion versus time data obtained by Borgwardt (1985). The kinetic data so obtained were the same to the obtained by using the UCM. In this case, the internal profiles of conversion and gas concentration were flat, as corresponding to an homogeneous reaction model.

4.3. Effect of particle size

Particle size has an important influence on the calcination rate of calcium based sorbents. For very small particles (1-90 μm), chemical reaction controls the calcination rate (Borgwardt, 1985; Milne, Silcox, Pershing & Kirchgessner 1990). Heat transfer becomes an important process for particle sizes above 6 mm (Rao et al., 1989). For particle sizes between them, chemical reaction and internal mass transfer are the main resistances that control the calcination. The relative importance of every one depends on the particle size and the porous structure of the sorbent. As an example, Figure 7 shows the influence of particle size on sorbent calcination for dolomite at atmospheric pressure. Similar results were obtained for the other sorbents. As expected, the calcination rate increased with decreasing particle size. This behaviour is consequence of the smaller importance of the pore diffusion as smaller is the particle size. This figure

also permits to observe the goodness of the model predictions using the kinetic and adsorption parameters previously obtained in this work. A good agreement between the experimental and model predictions was obtained for all sorbents and particle sizes.

4.4. Effect of total pressure

Calcium-based sorbents have been commonly used to remove gaseous pollutants in power plants. However, the most advanced processes, as the IGCC, normally operate with second-generation gasifiers at high pressure. In this work, calcination of the three sorbents was carried out at different operating conditions and pressures up to 1.5 MPa. Figure 8 shows an example of the conversion versus time curves obtained for half-calcined dolomite at different total pressures in nitrogen atmosphere. Similar trends were found for the other sorbents, although obviously with different reactivities. It was clear that calcination rate decreased with an increase in total pressure, even if there was no CO_2 in the reacting atmosphere. This effect was in fair agreement with the results reported by Dennis & Hayhurst (1987). These authors had accounted for this effect by assuming that the calcination rate was given by the following expression:

$$(r)_c \equiv \bar{k}\ S_e\left(P_{eq} - Py_1 - P_{CO_2}\right) = \bar{k}\ S_e\left(P'_{eq} - P_{CO_2}\right) \qquad (33)$$

where P is the total pressure, y_1 is a constant mole fraction of CO_2 which only depends on temperature, and $P'_{eq}=P_{eq}-Py_1$ is a spurious partial pressure of CO_2 at the equilibrium. They admitted that it was difficult to justify the use of a spurious partial pressure but it did account satisfactorily for their results. However, that expression was not valid to predict in our results the effect of total pressure for different CO_2 concentrations and particle sizes. Therefore, it seems more reasonable to think that the cause of the decrease on the reaction rate at higher pressures is due to an inhibition of gas diffusion. The gas diffusivity coefficient in a porous system is a combination of the Knudsen and molecular diffusivities. Knudsen diffusivity is not a function of total pressure, and the molecular diffusivity presents an inverse dependence on total pressure. In fact, a decrease of molecular diffusivity with increasing total pressure leads to a decrease on the effective gas diffusivity. A comparison between the experimental and simulated data with the kinetic parameters above obtained at atmospheric pressure is showed in Figure 8 as broken lines. Model predictions showed a small effect of total pressure on the calcination rate, far away of the great decrease experimentally obtained.

If the decrease in the calcination rate at increasing total pressure is certainly due to an inhibition of gas diffusion, and the porous system of the sorbents is not affected by total pressure, the molecular diffusivity should be more influenced by total pressure that the indicated by the Fuller's equation. It must be also taken into account that the majority of the data used by Fuller et al. (1966) to obtain their equation was obtained at or under atmospheric pressure. In this way, the molecular diffusivity could be calculated by a modified Fuller's equation:

$$D_{CO_2} = \frac{10^{-7}\, T^{1.75}\, (M_{CO_2}^{-1} + M_{N_2}^{-1})^{0.5}}{P^{m}\left[(\Sigma v)_{CO_2}^{1/3} + (\Sigma v)_{N_2}^{1/3}\right]^2} \qquad (34)$$

In our case, the parameter "m" was obtained by fitting the experimental pressurised data and the simulated from the particle models, SCM or CGSM, with the kinetic and sorption parameters above obtained at atmospheric pressure for the different sorbents. Surprisingly, the best fit was obtained for the same value of m, 1.6, for all the sorbents. The theoretical conversion versus time data obtained for the half-calcined dolomite is plotted with a continuous line in Figure 8. A good agreement between the experimental and simulated data can be observed. In the same way, very satisfactory results were also obtained for the other sorbents at different operating conditions. Figure 9 shows the effect of the CO_2 partial pressure on the calcination rate of Mequinenza limestone at 1 MPa of total pressure, and Figure 10 shows the effect of particle size on calcination rate at 1 MPa of total pressure and 0% CO_2. Finally, Figure 11 shows the effect of temperature on calcination rate at 0.6 MPa total pressure and 0% CO_2 for Blanca limestone. A good agreement between experimental and theoretical results was found in all the cases.

It must be finally remarked that neither the objective of this work was to find data on molecular diffusivity at high pressures, nor the experiments carried out were the most adequate for that. However, the use of the modified Fuller´s equation allowed us to adequately predict the effect of total pressure on the calcination reaction for sorbents of very different characteristics in a broad range of operating conditions.

5. Conclusions

SEM analysis of partially reacted particles demonstrated the existence of different sorbent behaviours during decomposition and allows to select the adequate solid reaction model to use in each case. SEM micrographs demonstrated that the decomposition of the Blanca limestone took place at a definite boundary between the CaO and $CaCO_3$ phases. However, the calcination of the Mequinenza limestone and the dolomite happened throughout all the particle, with different conversion levels at different particle locations. Therefore, the appropriate calcination models, the shrinking core model or the changing grain size model, must be used to determine the kinetic parameters of the sorbents.

The CO_2 partial pressure decreased the calcination rate. However, a sharp decrease in the calcination rate was found at the highest CO_2 concentrations. To adequately predict the sorbent conversion in all the range of CO_2 concentrations, several CO_2 partial pressure dependencies affecting the chemical reaction were tested. A Langmuir-Hinshelwood kinetic type model together with the Freundlich´s isotherm was valid to predict the experimental data in a broad range of CO_2 concentrations.

The above mentioned models were used to determine the kinetic and adsorption parameters for the different sorbents. The similar values obtained for the adsorption constants indicated that the adsorption process had the same characteristics independently of the sorbent. The activation energies herein determined were in the range of that obtained by other authors in similar operating conditions.

Pressurised calcination experiments showed that the calcination rate was affected by total pressure, even if there was no CO_2 in the reacting atmosphere. Other authors had also detected this effect of total pressure on several gas-solid reaction rates although no consistent reasons had been proposed. A detailed analysis of the possible causes of this effect indicated that the change in the effective gas diffusivity, and more specifically the molecular diffusivity, was the most probably reason for it. A higher dependence of the molecular diffusion coefficient on the total pressure with respect to that predicted by the Fuller's equation have to be assumed to adequately predict the experimental results carried out at pressure.

As conclusion, the developed models were valid to predict the calcination behaviour of very different calcium-based sorbents in a wide range of CO_2 concentrations, total pressures, particle size and temperatures.

Acknowledgement

This research was carried out with the financial support from the *Comisión Interministerial de Ciencia y Tecnología* (CICYT) (Project No. AMB 98-0883). The authors thank Dr. Diego Alvárez for his assistance with the SEM technique.

Notation

a exponential decay constant in equation (23) (-)

b exponent in equation (24) (-)

c adsorption constant in the Freundlich isotherm, equation (31) ($Pa^{-1/n}$)

c_0 preexponential factor of adsorption constant c ($Pa^{-1/n}$)

D dispersion coefficient ($m^2\ s^{-1}$)

D_e effective diffusivity within the particle ($m^2\ s^{-1}$)

D_g gas diffusion coefficient ($m^2\ s^{-1}$)

D_{CO_2} molecular diffusion coefficient of CO_2 ($m^2\ s^{-1}$)

D_K Knudsen diffusion coefficient ($m^2\ s^{-1}$)

d_p particle diameter (m)

E_a activation energy of adsorption constant c ($J\ mol^{-1}$)

E_c activation energy of chemical reaction rate constant ($J\ mol^{-1}$)

K_A adsorption constant in the Langmuir isotherm (Pa^{-1})

K_{eq} equilibrium constant for calcination reaction (Pa)

K_1 equilibrium constant for the chemical decomposition (-)

k_A adsorption rate constant ($mol\ m^{-2}\ s^{-1}\ Pa^{-1}$)

k_D desorption rate constant ($mol\ m^{-2}\ s^{-2}$)

k_c chemical reaction rate constant ($mol\ m^{-2}\ s^{-1}$)

k_g external mass transfer coefficient ($m\ s^{-1}$)

$\bar{k}$ rate constant for the CaO carbonation, equation (32), ($mol\ m^{-2}\ s^{-1}\ Pa^{-1}$)

k_0 preexponential factor of chemical reaction rate constant ($mol\ m^{-2}\ s^{-1}$)

k_1, k_2 kinetic constants for the chemical decomposition ($mol\ m^{-2}\ s^{-1}\ Pa^{-1}$)

L length of reactor (m)

M molecular weight ($g\ mol^{-1}$)

m total pressure exponent in equation (33) (-)

n number of active sites occupied by one molecule of CO_2 (-)

P total pressure (Pa)

P_{CO_2} CO_2 partial pressure (Pa)

P_{bulk} bulk CO_2 partial pressure (Pa)

P_{eq} equilibrium CO_2 partial pressure (Pa)

P'_{eq} spurious equilibrium partial pressure of CO_2 (Pa)

R radial coordinate within the particle (m)

R_0 particle radius (m)

R_c radius of shrinking core of calcium carbonate within the particle (m)

R_g ideal gas constant (J mol^{-1} K^{-1})

$(r)_c$ reaction rate of calcination (mol m^3 s^{-1})

$(r)'_c$ reaction rate of calcination (Pa s^{-1})

r_p pore radius (m)

r_0 initial grain radius (m)

r_2 radius of unreacted grain core (m)

Re_p particle Reynolds number (-)

S_e specific surface area (m^2 m^{-3})

S_g specific surface area (m^2 g^{-1})

S_0 initial specific surface area (m^2 m^{-3})

Sc Schmidt number (-)

Sh Sherwood number (-)

T temperature (K)

t time (s)

u gas velocity (m s^{-1})

V_M molar volume (m^3 mol^{-1})

X calcination conversion (-)

y_1 apparent mole fraction of CO_2 at the CaO-$CaCO_3$ interface (-)

Z stoichiometric volume ratio of solid product, CaO, to solid reactant, $CaCO_3$ (-)

Greek letters

ε particle porosity (-)

ε_0 initial particle porosity (-)

$(\Sigma v)_i$ diffusion volume for molecule i ($Å^3$)

ρ_r true density ($g\ m^{-3}$)

θ fraction of active sites occupied by CO_2 (-)

References

Barin, I. (1989). *Thermochemical data of pure substances*. Weinheim: VCH.

Borgwardt, R.H. (1985). Calcination kinetics and surface area of dispersed limestone particles. *A.I.Ch.E. Journal, 31*, 103-111.

Darroudi, T., & Searcy, A.W. (1981). Effect of CO_2 pressure on the rate of decomposition of calcite. *Journal of Physical Chemistry, 85*, 3971-3974.

Dennis, J.S., & Hayhurst, A.N. (1987). The effect of CO_2 on the kinetics and extent of calcination of limestone and dolomite particles in fluidised beds. *Chemical Engineering Science, 42*, 2361-2372.

Doraiswamy, L. K., & Sharma, M.M. (1984). *Heterogeneous Reactions*. New York: John Wiley & Sons.

Fuertes, A.B., Alvarez, D., Rubiera, F., Pis, J.J. & Marbán, G. (1991). Surface area and pore size changes during sintering of calcium oxide particles. *Chem. Eng. Comm*, *109*, 73-88.

Fuertes, A.B., Marbán, G., & Rubiera, F. (1993a). Kinetics of thermal decomposition of limestone particles in a fluidized bed reactor. *Transactions of I. Chem. E., 71(A)*, 421-428.

Fuertes, A.B., Alvarez, D., Rubiera, F., Pis, J.J., & Marbán, G. (1993b). Simultaneous calcination and sintering model for limestone particles decomposition. *Transactions of I. Chem. E., 71(A)*, 69-76.

Fuller, E.N., Schettler, P.D., & Giddings, J.C. (1966). A new method for prediction of binary gas-phase diffusion coefficients. *Industrial and Engineering Chemistry*, *58*, 19-27.

García-Calvo E., Arranz M.A., & Letón P. (1990) Effect of impurities in the kinetics of calcite decomposition. *Thermochimica Acta,170*, 7-11.

Georgakis, C., Chang, C.W., & Szekely, J. (1979). A changing grain size model for gas-solid reactions. *Chemical Engineering Science, 34*, 1072-1075.

Hashimoto, H. (1962). Thermal decomposition of calcium carbonate (II): effects of carbon dioxide. *Journal of Chemical Society of Japan, 64*, 1162-1165.

Hu, N., & Scaroni, A.W. (1996). Calcination of pulverized limestone particles under furnace injection conditions. *Fuel*, 75, 177-186.

Hyatt, E.P., Cutler, I.B., & Wadsworth, M.E. (1958). Calcium carbonate decomposition in carbon dioxide atmosphere. *Journal of American Ceramic Society, 41*, 70-74.

Ingraham, J.R., & Marier, P. (1963). Kinetic studies on the thermal decomposition of calcium carbonate. *Canadian Journal of Chemical Engineering, 41*, 170-173.

Khinast, J., Krammer, G.F., Brunner, Ch., & Staudinger, G. (1996). Decomposition of limestone: the influence of CO_2 and particle size on the reaction rate. *Chemical Engineering Science, 51,* 623-634.

Khraisha, Y.H., & Dugwell, D.R. (1989). Thermal decomposition of limestone in a suspension reactor. *Chemical and Engineering Research and Design, 67,* 52-57.

Matsukata, M., Ando, H., & Ueyama, K. (1999). Kinetics of CaO-H_2S reaction at high temperature under pressurized conditions. In Robert B. Reuther, *15th International Conference on Fluidized Bed Combustion* (FBC99-0009) Savannah: ASME.

Milne, C.R., Silcox, G.D., Pershing, D.W., & Kirchgessner, D.A. (1990). Calcination and sintering models for applications to high-temperature, short-time sulfation of calcium-based sorbents. *Industrial and Engineering Chemistry Research, 29,* 139-149.

Nelder, J.A., & Mead, R. (1964) A simplex method for function minimization. *Computer Journal, 7,* 308-313.

Ohme, K., Schrader, R., & Müller, A. (1975). Kinetik der thermischen Dissoziation von Kalkstein und Zamentrohmehl im Flugstaubreaktor. *Silikattechnik, 12,* 403-407.

Rao, T.R., Gunn, D.J., & Bowen, J.H. (1989). Kinetics of calcium carbonate decomposition. *Chemical Engineering Research Design, 67,* 38-47.

Schlichting, H. (1979). *Boundary layer theory* (7th ed.). New York: McGraw-Hill.

Silcox, G.D., Kramlich, J.C., & Pershing, D.W. (1989). A mathematical model for the flash calcination of dispersed $CaCO_3$ and $Ca(OH)_2$ particles. *Industrial and Engineering Chemistry Research, 28,* 155-160.

Wang, Y., & Thomson, W.J. (1995). The effects of steam and carbon dioxide on calcite decomposition using dynamic X-ray diffraction. *Chemical Engineering Science, 50,* 1373-1382.

Yrjas, P., Hupa, M., & Iisa K. (1996). Pressurized stabilization of desulfurization residues from gasification processes. *Energy and Fuels, 10,* 1189-1195.

Table 1. Chemical analysis and physical characteristics of the sorbents

	Blanca limestone	Mequinenza limestone	Sierra de Arcos dolomite
$CaCO_3$	97.1	95.8	52.5
$MgCO_3$	0.2	1.5	40.5
Others	2.7	2.7	7.0
Loss on decomposition (%)	44.0	44.4	40.6
$S_{g,CaCO3}$ (m^2 g^{-1}))	0.3	6.98	9.57*
$S_{g,CaO}$ (m^2 g^{-1}) **	19	19.4	30.4
$\varepsilon_{0,\ CaCO3}$	0.03	0.30	0.35*
ε_{CaO} **	0.56	0.68	0.57

* half-calcined

** Just after calcined at 900 ºC in nitrogen atmosphere.

Table 2. Kinetic and sorption parameters of calcination reaction.

	Blanca limestone	Mequinenza limestone	Sierra de Arcos dolomite
Chemical reaction			
E_c (kJ mol^{-1})	166	131	114
k_0 (mol m^{-2} s^{-1})	6.7 10^6	2.54 10^2	29.5
Adsorption mechanism			
E_a (kJ mol^{-1})	-93	-90	-90
c_0 ($Pa^{-0.5}$)	$1.8 \cdot 10^{-7}$	3.7 10^{-7}	3.5 10^{-7}

Captions of the Figures

Figure 1. Effect of external mass transfer and interparticle diffusion working at pressure. (Blanca limestone, 1123 K, 0.5 MPa, dp= 0.8-1 mm).

Figure 2. SEM pictures of the partially calcined sorbents. a) particle of Blanca limestone; b) Interface between $CaCO_3$ and CaO in Blanca limestone; c) Mequinenza limestone (external zone); d) Mequinenza limestone (internal zone); e) particle of Sierra de Arcos dolomite; and f) internal view of the dolomite particle.

Figure 3. Effect of CO_2 partial pressure on the calcination conversion for the three sorbents: symbols, experimental data; continuous line, model predictions (0.1 MPa)

Figure 4. Effect of CO_2 partial pressure on the calcination conversion for the Blanca limestone. (1173 K, 0.1 MPa, dp=0.8-1 mm). Continuous line, a = 4 in eq. (23); broken line, b = 2 in eq. (24).

Figure 5. Temperature dependence of the kinetic constant for the sorbents used and comparison with data of Borgwardt (1985) and Fuertes et al. (1993a).

Figure 6. Temperature dependence of the adsorption parameters for the sorbents used.

Figure 7. Effect of particle size on the calcination rate of the half-calcined Sierra de Arcos dolomite: symbols, experimental data; continuous line, model predictions. (1123 K, 0% CO_2, 0.1 MPa).

Figure 8. Effect of total pressure on the calcination conversion of the half-calcined Sierra de Arcos dolomite: symbols, experimental data; broken line, model predictions with Fuller`s equation; continuous line, model predictions with equation (34) and m=1.6. (1123 K, 0% CO_2, dp = 0.8-1 mm).

Figure 9. Effect of CO_2 partial pressure on the calcination conversion of Mequinenza limestone: symbols, experimental data; continuous line, model predictions. (1123 K, 1 MPa, dp=0.8-1 mm)

Figure 10. Effect of particle size on the calcination conversion of Mequinenza limestone: symbols, experimental data; continuous line, model predictions. (1123K, 1 MPa, 0% CO_2).

Figure 11. Effect of temperature on the calcination conversion of Blanca limestone: symbols, experimental data; continuous line, model predictions. (0.6 MPa, 0% CO_2, dp = 0.8-1 mm).

Calcination of calcium-based sorbents at pressure in a broad range of CO_2 concentrations

F. García-Labiano et al.

Figure 1

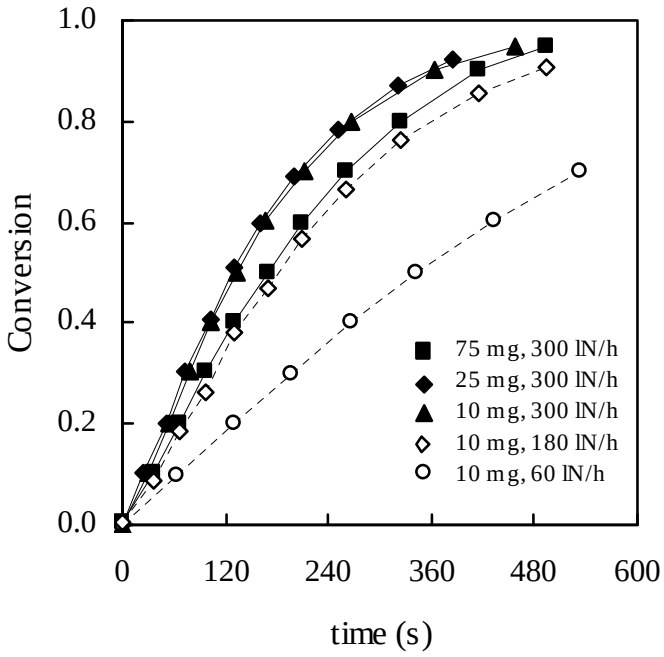

Calcination of calcium-based sorbents at pressure in a broad range of CO_2 concentrations

F. García-Labiano et al.

Figure 2

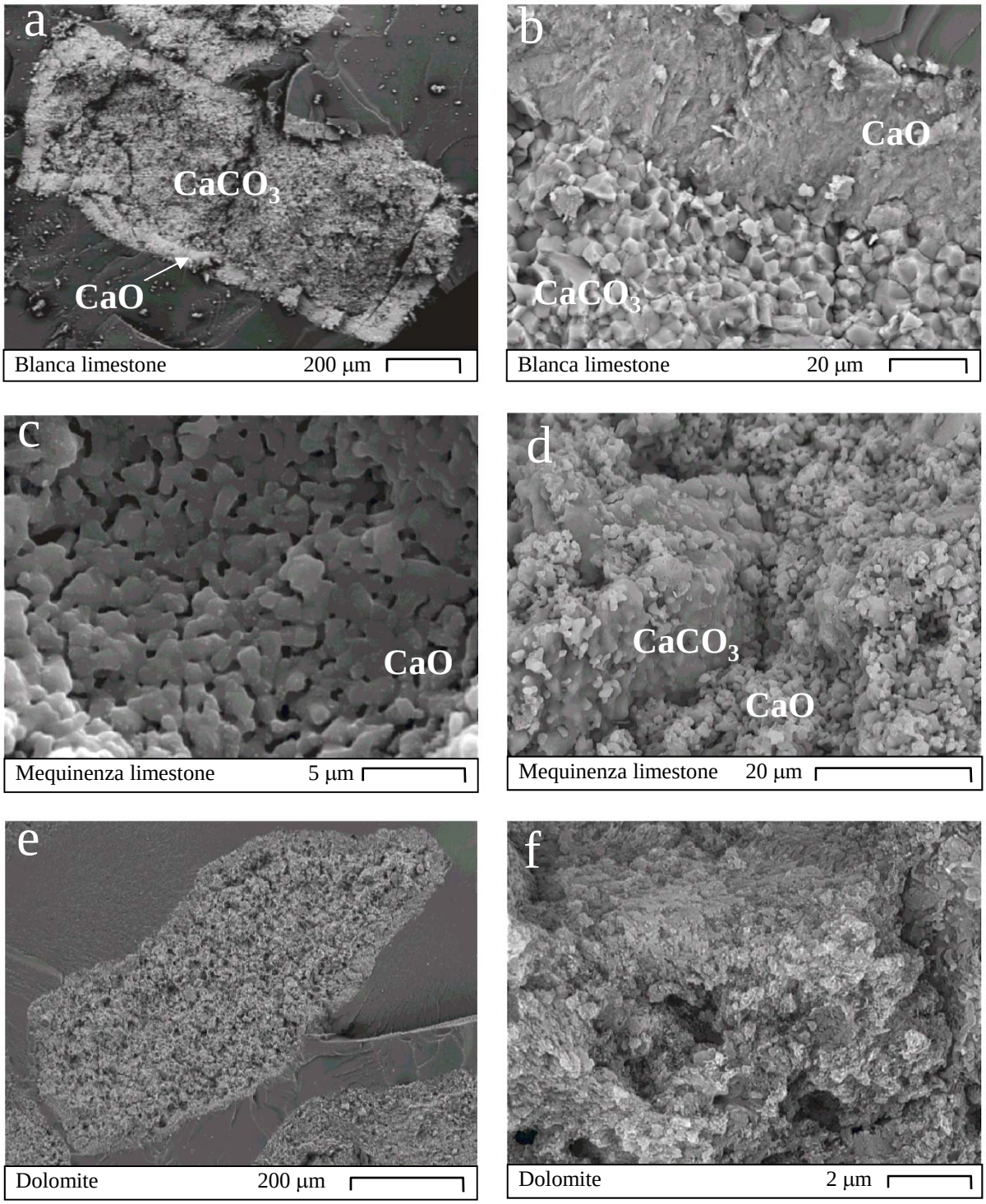

Calcination of calcium-based sorbents at pressure in a broad range of CO_2 concentrations

F. García-Labiano et al.

Figure 3

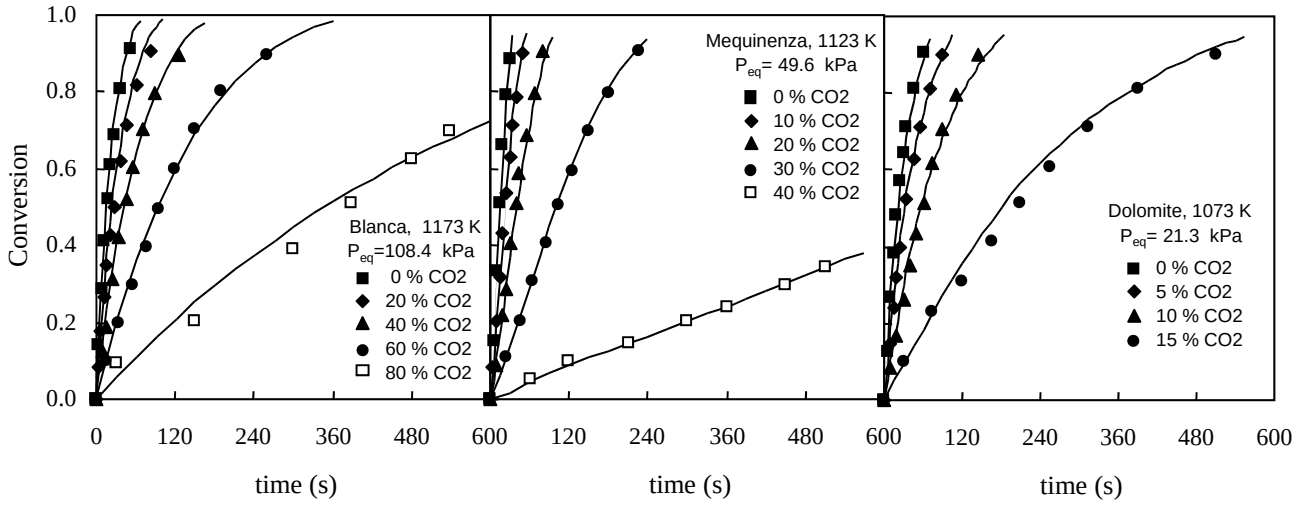

Calcination of calcium-based sorbents at pressure in a broad range of CO_2 concentrations

F. García-Labiano et al.

Figure 4

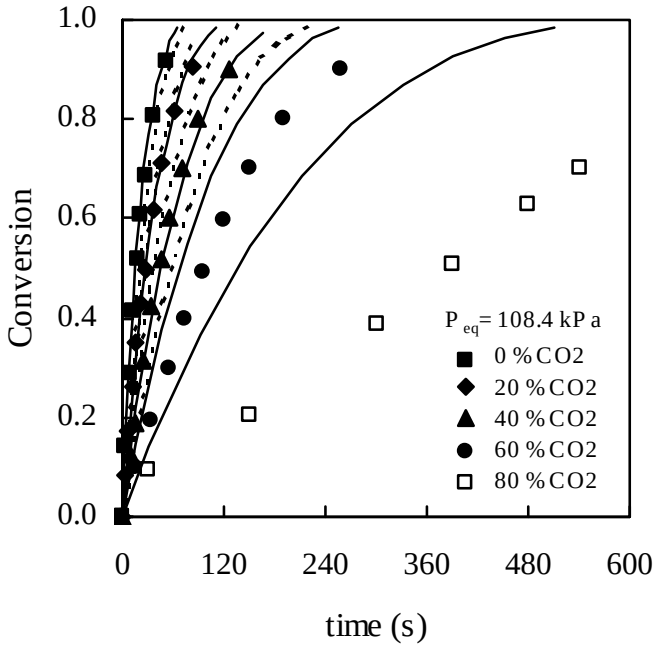

Figure 5

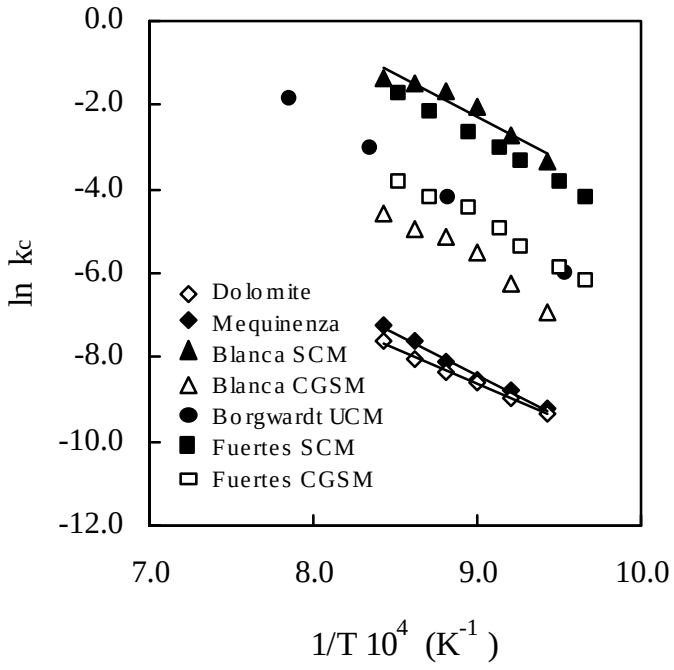
0.0
-2.0
-4.0
-6.0
-8.0
-10.0
-12.0
ln kc
7.0
8.0
9.0
10.0
1/T 10^4 (K^-1)
Dolomite
Mequinenza
Blanca SCM
Blanca CGSM
Borgwardt UCM
Fuertes SCM
Fuertes CGSM

Figure 6

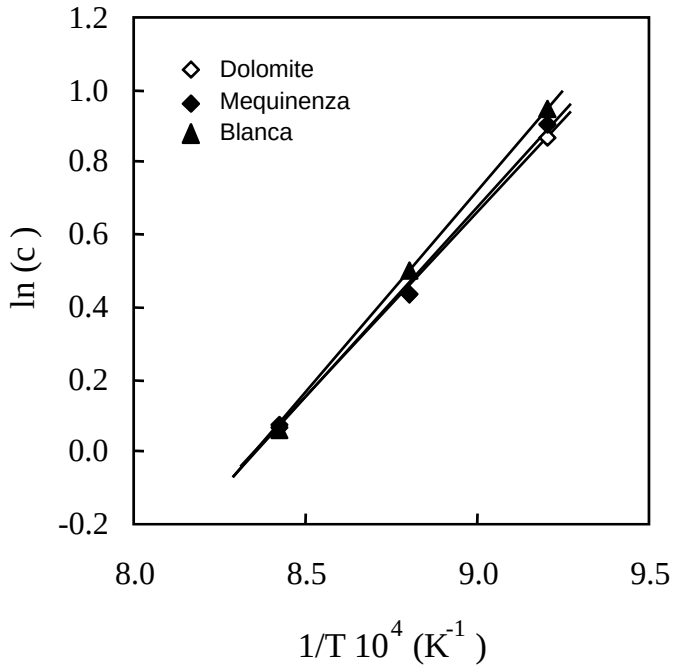
1.2
1.0
0.8
0.6
0.4
0.2
0.0
-0.2
ln (c)
Dolomite
Mequinenza
Blanca
8.0
8.5
9.0
9.5
1/T 10^4 (K^-1)

Figure 7

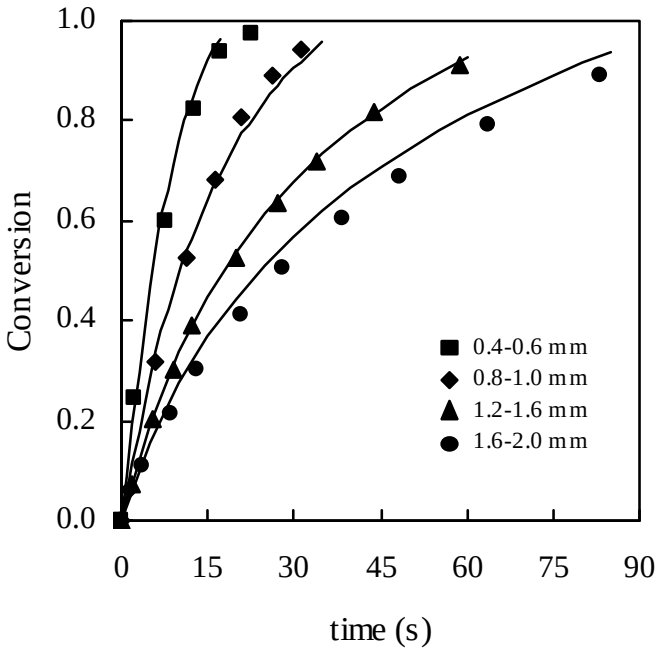
1.0
0.8
0.6
0.4
0.2
0.0
Conversion
0
15
30
45
60
75
90
time (s)
0.4-0.6 mm
0.8-1.0 mm
1.2-1.6 mm
1.6-2.0 mm

Calcination of calcium-based sorbents at pressure in a broad range of CO_2 concentrations

F. García-Labiano et al.

Figure 8

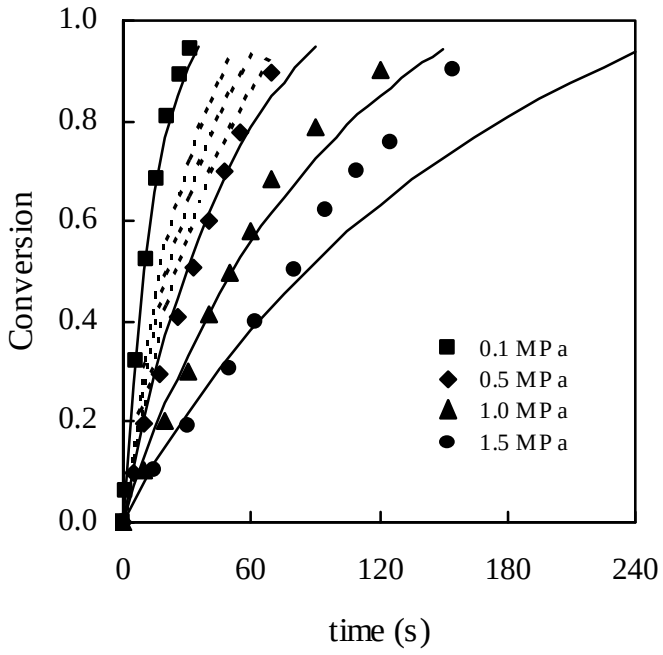

Calcination of calcium-based sorbents at pressure in a broad range of CO_2 concentrations

F. García-Labiano et al.

Figure 9

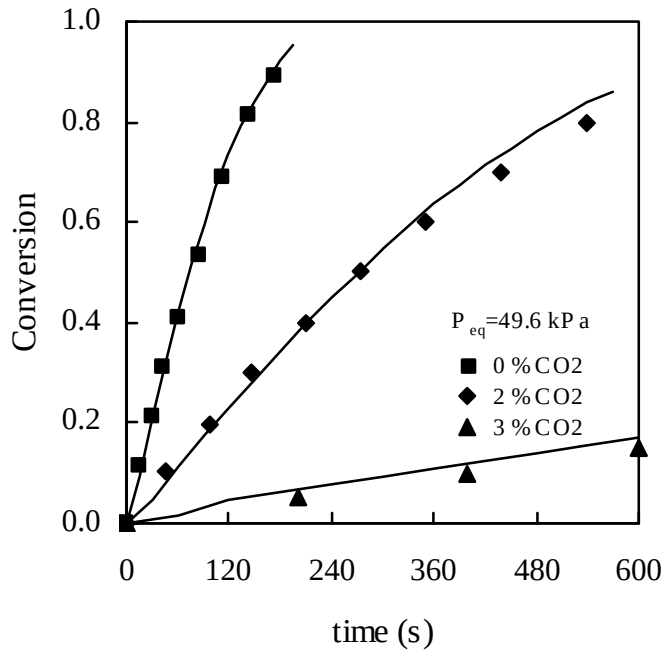

Figure 10

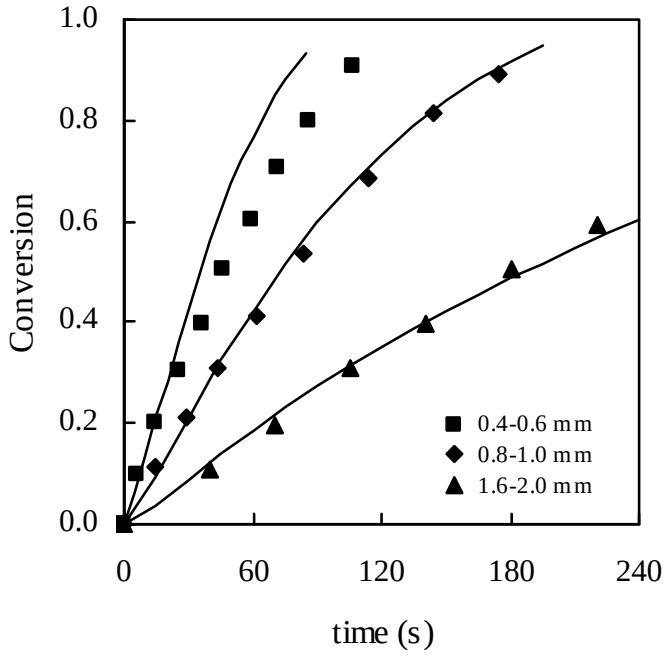
1.0
0.8
0.6
0.4
0.2
0.0
Conversion
0
60
120
180
240
time (s)
0.4-0.6 mm
0.8-1.0 mm
1.6-2.0 mm

Figure 11

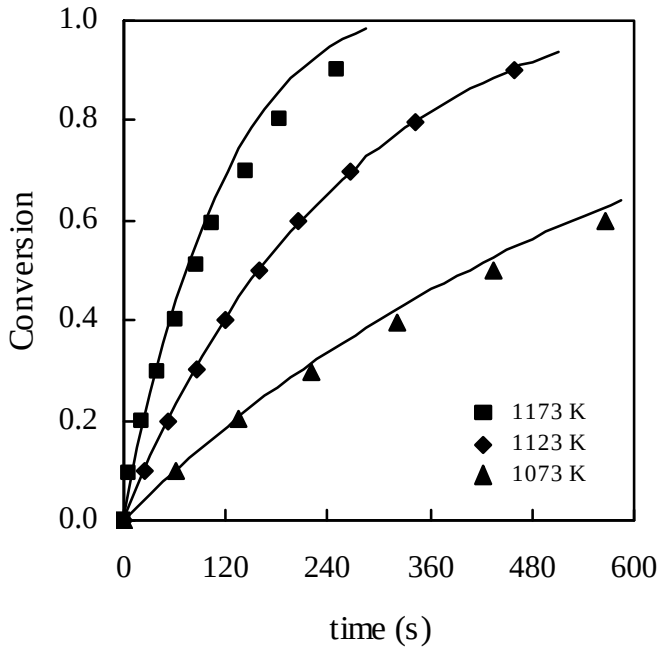
1.0
0.8
0.6
0.4
0.2
0.0
Conversion
0
120
240
360
480
600
time (s)
1173 K
1123 K
1073 K